Trends in Biochemical Sciences

CellPress OPEN ACCESS

Review

Structural mechanisms of mitochondrial uncoupling protein 1 regulation in thermogenesis

Scott A. Jones [1], Jonathan J. Ruprecht [1], Paul G. Crichton [2], and Edmund R.S. Kunji [1,*]

In mitochondria, the oxidation of nutrients is coupled to ATP synthesis by the generation of a protonmotive force across the mitochondrial inner membrane. In mammalian brown adipose tissue (BAT), uncoupling protein 1 (UCP1, SLC25A7), a member of the SLC25 mitochondrial carrier family, dissipates the protonmotive force by facilitating the return of protons to the mitochondrial matrix. This process short-circuits the mitochondrion, generating heat for non-shivering thermogenesis. Recent cryo-electron microscopy (cryo-EM) structures of human UCP1 have provided new molecular insights into the inhibition and activation of thermogenesis. Here, we discuss these structures, describing how purine nucleotides lock UCP1 in a proton-impermeable conformation and rationalizing potential conformational changes of this carrier in response to fatty acid activators that enable proton leak for thermogenesis.

Highlights

Uncoupling protein 1 (UCP1, SLC25A7) is a mitochondrial carrier that facilitates thermogenesis in brown adipose tissue (BAT) by dissipating the protonmotive force and is a potential target for therapeutics against metabolic disease.

Recent cryo-electron microscopy (cryo-EM) structures of human UCP1 have provided molecular insights into pH-dependent purine nucleotide inhibition of thermogenesis in BAT.

UCP1 has the structural fold of members of the SLC25 mitochondrial carrier family, suggesting a related mechanism involving conformational changes, required to initiate proton conductance.

The chemical uncoupler 2,4-dinitrophenol (DNP), which binds weakly to UCP1, does not induce conformational changes and retains a proton-impermeable state.

Analysis of the structural features reveals potential molecular components of an activation mechanism of UCP1 in thermogenesis.

Thermogenesis and UCP1

To support thermoregulation, many mammals, particularly newborns, use specialized fat deposits, known as **BAT (**see Glossary), to carry out **non-shivering thermogenesis** to protect against cold temperatures [1–3]. BAT is distinct from white adipose tissue due to its higher density of mitochondria, larger number of blood vessels, and smaller fat deposits. Heat generation by BAT occurs due to the presence of mitochondrial **UCP1**, also called thermogenin. The oxidation of breakdown products from fats and sugars is used by the complexes of the mitochondrial electron transport chain to generate a **protonmotive force**, which is used for ATP synthesis (Figure 1A). However, UCP1 short-circuits the mitochondrion by allowing protons to leak back from the intermembrane space to the mitochondrial matrix, dissipating the protonmotive force, which generates heat rather than chemical energy in the form of ATP (Figure 1A).

The activity of UCP1 is tightly controlled by regulatory ligands. Cytosolic **purine nucleotides** bind with high affinity to UCP1 to inhibit proton leak activity [4–6]. However, a cold environment induces sympathetic nerve activity and the adrenergic stimulation of BAT, leading to UCP1 activation. Intracellular signaling within brown adipocytes results in the phosphorylation of hormone-sensitive lipase and perilipin, lipolysis of triglyceride stores, and the release of free fatty acids [7]. These **fatty acid activators** directly interact with UCP1 [8], stimulating proton leak across the mitochondrial inner membrane by a mechanism that is as yet unresolved [9].

UCP1 activation is of therapeutic interest as it can help increase calorie expenditure and the clearance of triglycerides and glucose from the bloodstream [10,11]. Human brown fat correlates inversely with age-related obesity [12–14] and, when activated, improves insulin sensitivity and glucose homeostasis [15]. Recently, several atomic structures of UCP1 were determined by

[1]MRC Mitochondrial Biology Unit, University of Cambridge, Cambridge Biomedical Campus, Keith Peters Building, Cambridge, CB2 0XY, UK
[2]Biomedical Research Centre, Norwich Medical School, University of East Anglia, Norwich, NR4 7TJ, UK

*Correspondence: ek@mrc-mbu.cam.ac.uk (E.R.S. Kunji).

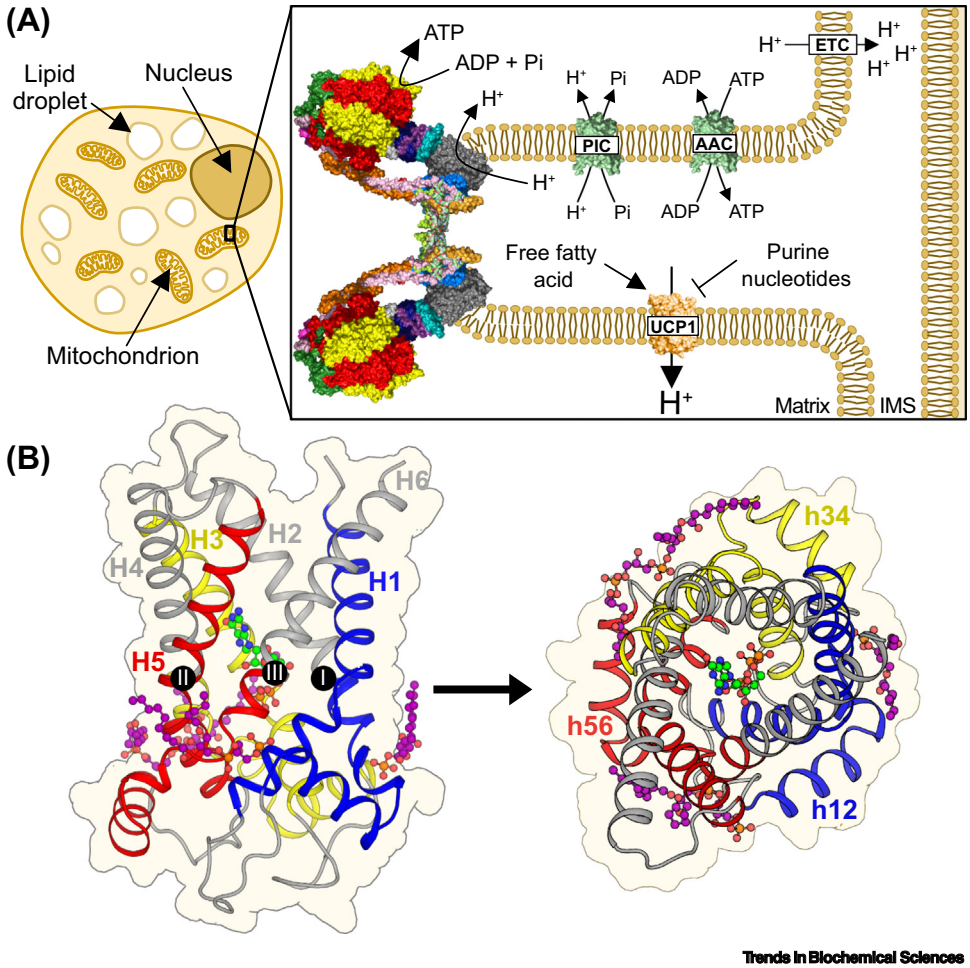

Figure 1. Physiological role and structure of uncoupling protein 1 (UCP1). (A) Brown adipose tissue cell (left). Mitochondrial membranes (right) showing a crista with ATP synthase at the tip with the phosphate carrier (PIC), ADP/ATP carrier (AAC), UCP1, and electron transport chain (ETC) within the mitochondrial inner membrane. UCP1 dissipates the protonmotive force across the inner mitochondrial membrane, which is activated by free fatty acids and inhibited by purine nucleotides. (B) Structure of UCP1 (PDB ID: 8G8W chain A) [16]. Lateral (left) and cytoplasmic (right) view with bound GTP (green) and three cardiolipin molecules (purple). Substrate binding in mitochondrial carriers occurs at the contact point residues (black circles), which are situated between the core (blue, yellow, and red helices) and gate elements (gray helices). The core and gate elements undergo substantial conformational changes during c- to m-state interconversion.

cryo-EM, revealing the molecular details of the protein for the first time [16,17]. In this review, we discuss the new molecular insights into the inhibition and activation mechanisms of UCP1. Understanding these is vital for the advancement of therapeutic strategies to stimulate thermogenesis for the treatment of obesity and associated metabolic diseases.

UCP1 is a mitochondrial carrier

UCP1 (SLC25A7) is a member of the SLC25 **mitochondrial carrier** family, which is the largest transporter family in humans. Most mitochondrial carriers are involved in metabolite transport across the mitochondrial inner membrane [18]. SLC25 members are defined by three homologous domains, each comprising two transmembrane α-helices separated by a loop and a matrix helix (Figure 1B). Studies of the mitochondrial ADP/ATP carrier, another member of the SLC25

Glossary

Brown adipose tissue (BAT): specialized fat tissue found in mammals that contains mitochondria with UCP1 expressed at high levels. When exposed to cold temperatures, mitochondria in BAT uncouple oxidative phosphorylation from ATP synthesis to generate heat and maintain body temperature.
Chemical uncouplers: compounds that carry protons across biological membranes, dissipating the protonmotive force generated by the electron transport chain, which removes the driving force for ATP synthase.
Contact points: amino acid residues on the even-numbered transmembrane helices of mitochondrial carriers, including UCP1, involved in substrate binding and coupling to conformational changes.
Cytoplasmic network: salt bridge network on the cytoplasmic side of a carrier protein, which closes the central cavity and substrate-binding site to the intermembrane space when formed, holding the carrier in a m-state conformation. The network is highly conserved in mitochondrial carriers.
Cytoplasmic state (c-state): conformation of mitochondrial carriers where the central substrate-binding site is accessible from the cytoplasm.
2,4-Dinitrophenol (DNP): protonophore that disrupts the protonmotive force across the mitochondrial inner membrane by transporting protons.
Fatty acid activators: free fatty acids generated from lipolysis of stored triglycerides in response to cold exposure, which are known activators of proton conductance by UCP1 and, therefore, thermogenesis in BAT.
Matrix network: salt bridge network formed on the matrix side of UCP1, observed in all UCP1 structures, which holds the protein in a c-state closed to the mitochondrial matrix.
Matrix state (m-state): conformation of mitochondrial carriers where the central substrate-binding site is open to the mitochondrial matrix.
Mitochondrial carrier: group of transporters of the SLC25 family that transport metabolites and ions across the mitochondrial inner membrane.
Nanobodies or sybodies: single-domain antibodies raised to bind folded protein epitopes specifically, which aide structural determination by cryo-EM or X-ray crystallography.

family, revealed the fundamental transport mechanism of mitochondrial carriers [19–21]. These carriers cycle between two conformations: one open to the intermembrane space, which is confluent with the cytoplasm (**cytoplasmic state; c-state**) [22,23] and another open to the mitochondrial matrix (**matrix state; m-state**) [24]. The conformational changes are coupled to the formation and disruption of two networks on either side of the carrier, which are part of the access gates to a central substrate-binding site [25]. The binding site comprises three **contact points** on the even-numbered transmembrane helices [26,27]. In the c-state, the residues of the matrix salt bridge network [22] and glutamine braces [23] interact, closing the central cavity to the matrix, whereas the residues of the cytoplasmic salt bridge network and tyrosine braces are not [24], opening the carrier to the intermembrane space. In the m-state, the configurations of the two networks are switched, opening the carrier to the mitochondrial matrix [24]. The conformational changes involve all three domains, each comprising a core and a gate element [24]. When the carrier changes from the c-state to the m-state, the three core elements rotate outward, opening the matrix side, whereas the three gate elements rotate inward, closing the cytoplasmic side of the carrier [24]. The same elements operate in reverse when the carrier moves from the m-state to the c-state.

Cryo-EM structures of human UCP1

Determining protein structures by cryo-EM is challenging for proteins <100 kDa [28], but UCP1 is particularly difficult due to its small size (33 kDa), the presence of three pseudo-symmetrical domains, and its dynamic nature. Therefore, to facilitate its structure determination, fiducial markers were used to increase both the size and asymmetry of the protein. **Nanobodies** or synthetic nanobodies (**sybodies**) are attractive fiducials, because they are single-chain antibody fragments that can bind conformational epitopes and stabilize states [29,30]. Since nanobodies are small (15 kDa), they need to be enlarged, either by creating a fusion protein, such as a Promacrobody [31], or by creating protein complexes, such as legobodies [32]. Both strategies enabled the processing of particle images, taken by cryo-EM, to generate a density map of sufficient resolution for the building of atomic models of UCP1.

Structures of human UCP1 were solved in the GTP-bound state (PDB ID: 8G8W), ATP-bound state (PDB ID: 8HBW), and unliganded state (PDB ID: 8HBV), as well as in a **2,4-dinitrophenol** (**DNP**; a proposed activator [33])-bound state (PDB ID: 8J1N) [16,17]. The structures show that UCP1 has a typical fold for a SLC25 family member [20] and that the protein is monomeric with three bound cardiolipin molecules [16] (Figure 1B), as determined previously [34]. Notably, all solved structures used nanobodies or sybodies selected against the nucleotide-bound state of UCP1. While the amino acid numbering differs between the deposited structures, 8G8W follows the Uniprot sequence (P25874), which is also used here. These structures revealed the molecular properties of UCP1 for the first time, enabling analysis of the molecular mechanisms that control non-shivering thermogenesis in humans.

Purine nucleotides lock UCP1 in a proton-impermeable configuration

The structures of UCP1 with bound GTP [16] and ATP [17] have revealed how purine nucleotides inhibit UCP1, preventing proton leak. The independently solved nucleotide-bound UCP1 structures are very similar [**root mean squared deviation (RMSD)**: 0.86 Å] despite using distinct lipidic mimetic systems (detergent and nanodiscs) and fiducial markers that bind to different epitopes [16,17,29]. Purine nucleotides bind in the central cavity of UCP1 and lock the protein in a conformation that is open to the cytoplasm (c-state). Given the similarities between the chemical structures of ATP and GTP, most interactions are conserved. The binding arrangement accounts for their comparable affinities, although GTP has a slightly lower K_D in radiolabeled nucleotide-binding experiments compared with ATP [35]. The triphosphate and ribose groups

Non-shivering thermogenesis: physiological process in which heat is generated through the dissipation of the protonmotive force produced by oxidative phosphorylation in BAT, rather than through shivering muscle contractions.
Protonmotive force: membrane potential and pH difference across inner mitochondrial membrane generated by the proton pumps of the electron transport chain, which is used for ATP synthesis and other cellular processes, such as transport.
Purine nucleotides: phosphorylated ribose bonded to purine bases, such as guanine and adenine, which comprise fused pyrimidine and imidazole rings.
Root mean squared deviation (RMSD): measure of the structural similarity of two proteins, quantifying the average deviation of atom positions.
Uncoupling protein 1 (UCP1): mitochondrial carrier (SLC25A7) responsible for dissipating the protonmotive force generated across the mitochondrial inner membrane during oxidative phosphorylation, short-circuiting the mitochondrion and causing thermogenesis.

of both purine nucleotides have similar interactions with UCP1 (Figure 2A,B). The triphosphate group forms electrostatic interactions with the positively charged central cavity comprising contact point residues R84, R277, and R183 (the 'arginine triplet') [26,27] and **matrix network** residues K38 and K138. In addition, Q85 forms a hydrogen bond with the α-phosphate and R183 forms a hydrogen bond with the ribose group. R92 forms a cation-π interaction with both adenine and guanine heterocyclic rings. The interactions of the nucleotides with UCP1 differ at the base: adenine forms hydrogen bonds with two asparagine residues, connecting N_6 with N188 and N_3 with N282 (Figure 2A); by contrast, the N_2 of guanine interacts electrostatically with E191, whereas N_3 and N_2 form hydrogen bonds to N188 (Figure 2B).

Notably, nucleotide binding to UCP1 [16,17] differs fundamentally from ATP binding to the mitochondrial ADP/ATP carrier (AAC) [36] in agreement with ATP being an inhibitor of UCP1 and a transport substrate of AAC [4,37]. In mitochondrial carriers, substrate binding primarily occurs at the contact points [26,27], which also act as hinges between the core and gate elements, which undergo large conformational changes between the c- and m-states [24,26,36]. In the mitochondrial ADP/ATP carrier, both the triphosphate and adenine groups interact with the contact point residues to disrupt one salt bridge network and form another, leading to substrate translocation [36]. In UCP1, purine nucleotides interact not only with the contact points, but also with the matrix network and gate elements, as well as with residues toward the cytoplasmic side of the cavity, explaining how they act as inhibitors, preventing conformational changes [16].

The UCP1 structures reveal an unusual state-dependent distortion on transmembrane helix H2. In the unliganded UCP1 structure, residues 92–96 form a π-bulge (Figure 2C), where the standard main-chain *i*, *i*+4 hydrogen bonding is changed to *i*, *i*+5. By contrast, in the GTP- and ATP-inhibited structures, residues 92–96 form a standard α-helix, but residues 85–89 adopt a π-bulge (Figure 2D). As a result, the main-chain carbonyl oxygen of S87 misses a hydrogen bond donor and rotates toward the membrane (Figure 2E). The switch from a π- to α-helical arrangement in the region of R92 induces localized rotation of the main chain (Figure 2F). Consequently, R92 moves from interacting with M285 and F289 (both on helix H6) in the unliganded state to interacting directly with the α-phosphate and purine base of the inhibitor in the bound state (Figure 2F). Consistent with this notion, π-bulges in helices are frequently located in functionally important sites, and transformations between α- and π-helical arrangements have been proposed to help active sites accommodate ligands of different shapes and sizes [38]. Superimposition of the three domains of UCP1 for the nucleotide-bound and unliganded state shows movement of the gate element of transmembrane H2. A similar movement occurs during c- and m-state conversion of the ADP/ATP carrier and suggests that UCP1 is in an intermediate state when inhibited by nucleotides [16,24]. Otherwise, the unliganded state is very similar to the nucleotide-bound state and is also likely to be proton impermeable, having a closed matrix gate preventing the leak of protons.

A plausible molecular explanation for the pH-dependence of purine nucleotide binding

The binding affinity of purine nucleotides to UCP1 is pH dependent (Figure 3A) and decreases above pH 6.5 [16,35,37,39]. Previously, residue E191 was proposed to be responsible for the pH dependency of nucleotide binding [40–42], and was suggested to form an ionic bond with R92 [43]. Above pH 6.5, this interaction would block nucleotide binding [44], whereas, below pH 6.5, the ionic bond would be broken by protonation, opening the site for nucleotide binding [6,39,45]. This interaction has been observed in molecular dynamics simulations of a c-state model of UCP1, based on the ADP/ATP carrier [46]. However, E191 is not in bonding distance with R92 in the unliganded state structure (11.3 Å) [17], even when all alternative conformers are

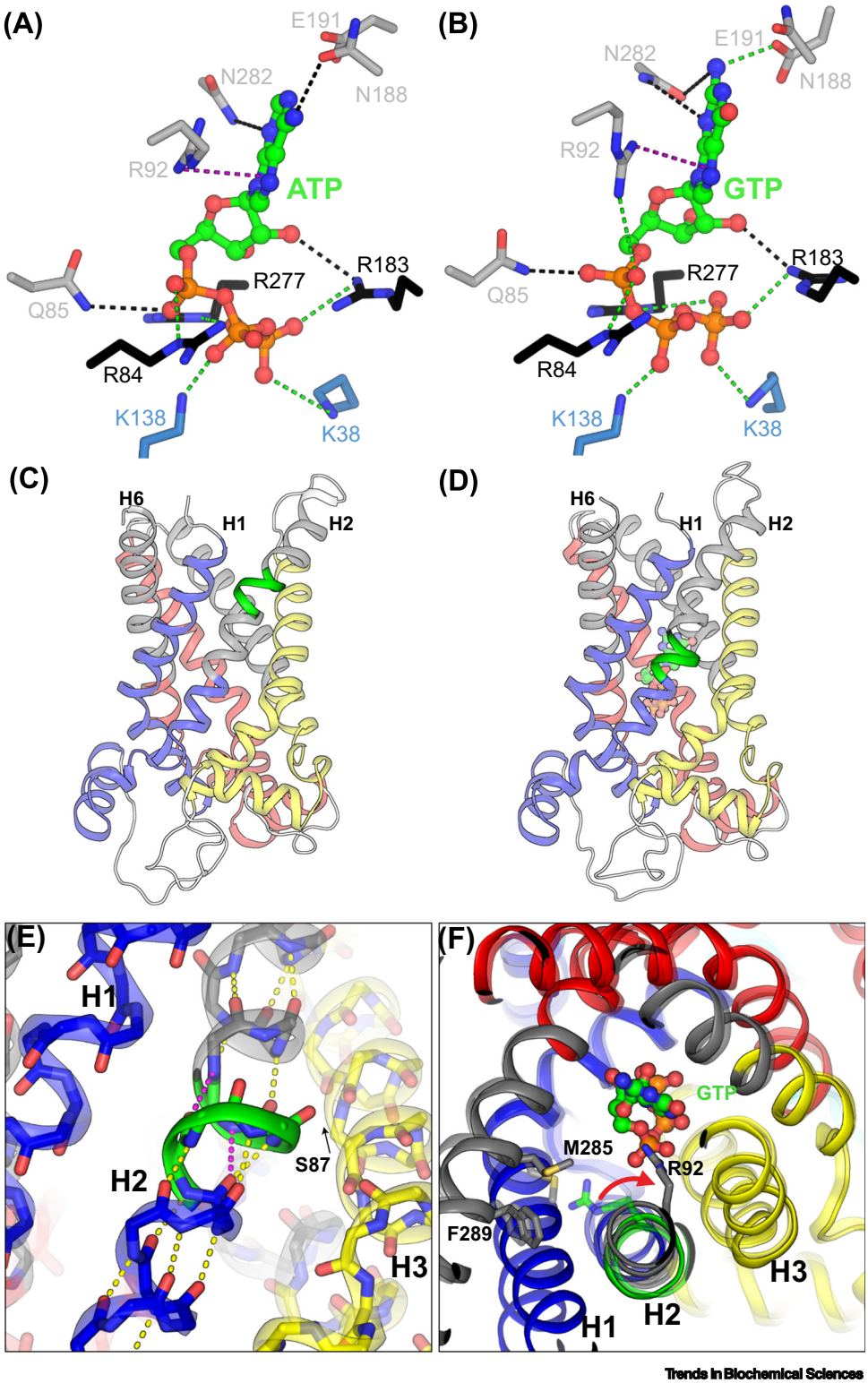

(See figure legend at the bottom of the next page.)

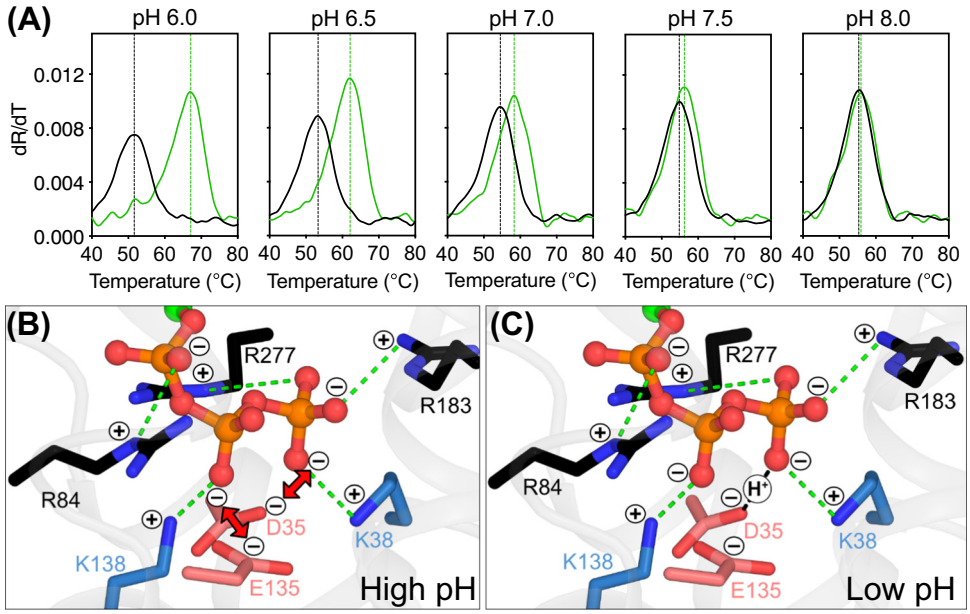

Figure 3. The pH dependency of purine nucleotide inhibition of uncoupling protein 1 (UCP1). (A) The pH-dependent binding of GTP to purified human UCP1, as measured by a thermal stability shift assay [16]. The first derivatives of the unfolding curves are plotted in the absence (black) and presence of 1 mM GTP (green). The peak of the first derivative is the apparent melting temperature (Tm). The change in apparent melting temperature (ΔTm) caused by GTP binding as a function of pH is indicated in green. (B) Nucleotide binding at high pH, showing the negatively charged residues of the matrix gate (in red) repelled (red arrows) by the negatively charged phosphate groups of the nucleotide (in orange and red). (C) Nucleotide binding at low pH, showing the negatively charged residues of the matrix gate (in red) interacting via a proton-mediated bond to the terminal phosphate group of the nucleotide (in orange and red).

considered. Indeed, in simulations, substantial distortion of the helical arrangement is required for this bond to occur [46]. Furthermore, E191 would not be protonated unless the local pH is <4, which does not match the pH-dependent profile of nucleotide binding. Importantly, E191 does interact with GTP [16], but not with ATP (Figure 2A) [17], even though the pH effect is observed for both nucleotides [6]. In agreement, the E191Q mutation weakens binding, but does not abolish the pH dependency of GTP binding [41], indicating that there must be an alternative explanation.

Both nucleotide-bound structures show that the negatively charged D35 and E135 of the matrix gate are positioned within bonding distance of the negatively charged triphosphate moiety of the purine nucleotides, which, at high pH, could cause repulsion (Figure 3B), but, at low pH, could form proton-mediated bonds (Figure 3C) [16]. The nucleotide-binding site has net negative overall

Figure 2. Purine nucleotide binding to uncoupling protein 1 (UCP1). (A) ATP (green) binding site (PDB ID: 8HBW chain A). The arginine triplet residues are shown in black; matrix network residues are shown in blue, and other residues involved in nucleotide binding are shown in gray. Salt bridge, hydrogen bond, and cation-π interactions are shown in green, black, and purple broken lines, respectively. (B) GTP (green) binding site (PDB ID: 8G8W chain A). Residues and interactions are depicted as in (A). (C) Unliganded UCP1 (PDB ID: 8HBV chain A) shown in cartoon representation, as in Figure 1B in the main text, but with the π-helix on H2 represented in green. (D) GTP-inhibited UCP1 (PDB ID: 8G8W chain A) shown as in (C). (E) Close-up view of the π-helix shown in (C), with mainchain atoms shown in stick representation. Conventional *i*, *i*+4 hydrogen-bonds are shown as yellow broken lines, and π-helix *i*, *i*+5 hydrogen-bonds are shown as magenta broken lines. (F) Comparison of uninhibited UCP1 (semitransparent cartoon) and GTP-inhibited UCP1 (opaque cartoon) showing the localized main-chain rotation (red arrow) and shift in the position of R92, which allows the residue to interact with the guanine base and α-phosphate of GTP.

charge and, thus, neutralizing this charge with protons will lead to stronger binding of the nucleotide. One proton could mediate bonding between the terminal phosphate and D35, in agreement with the pKa of 6.5 for purine nucleotides in solution (Figure 3C). However, in this conjugated system, another proton could also be drawn in to provide an additional proton-mediated interaction with E135. This bonding arrangement provides a plausible molecular mechanism for the pH dependency of purine nucleotide binding to UCP1.

The dinitrophenol-bound structure does not resolve the activation mechanism of UCP1

Weak acids can transport protons across biological membranes [47] and can function in mitochondria as **chemical uncouplers** by acting as protonophores, dissipating the protonmotive force. DNP is a well-known chemical uncoupler, which was used as weight-loss medication during the 1930s because of its ability to uncouple mitochondria [48]. However, the compound is highly toxic due to its unpredictable accumulation and distribution, which can lead to dangerous levels of oxidative phosphorylation inhibition [49]. Even though banned, DNP is still used as a weight loss agent, causing numerous deaths [49,50]. It was recently reported that UCP1 mediates DNP-induced proton leak across the mitochondrial inner membrane, which was abolished in mitochondria from UCP1-knockout animals [33].

Kang and Chen solved a UCP1 structure with bound DNP, used as an 'activator', by using the same sybody that was selected against the nucleotide-bound inhibited state [17]. The authors reported that DNP binds with extremely low potency, with an IC_{50} of 3.86 mM being measured for DNP-induced destabilization of UCP1; thus, a concentration of 10 mM DNP was utilized in the study. Despite using a high DNP concentration, only ~42% of 3D classes showed density for DNP during cryo-EM reconstruction, meaning that the K_D must be >10 mM [17]. In the structure, DNP binds to UCP1 via hydrogen bonds between R92 and R84 and N_4, a hydrogen bond between N282 and N_2, an ionic bond between R277 and the hydroxyl group, and a π-π stacking interaction between W281 and the benzene ring of DNP (Figure 4A). Importantly, DNP does not induce any significant structural alterations, as the RMSD between unliganded and DNP-bound UCP1 is 0.25 Å. In addition, the central cavity is closed to the mitochondrial matrix with a large proton-impermeable layer similar to the unliganded and nucleotide-bound states (Figure 4B). As such, there is no structural evidence to support the hypothesis that DNP binding generates a proton-conducting state. Therefore, Kang and Chen propose that UCP1 is activated when bound to DNP by dynamic thermal motions, which transiently open the matrix gate to allow protons to pass through the central cavity [17]. However, there are several problems with this proposal.

First, DNP is chemically distinct and not a clear surrogate for fatty acids, the physiological activators, and may utilize a different mechanism. In addition, at the high concentrations used, DNP may bind to a UCP1 site that is unrelated entirely to the activation mechanism by either class of compounds. Moreover, the sybody was raised against the nucleotide-inhibited state and may restrict alternative activator-accessible conformations. Notably, the destabilization by DNP reported by the authors [17] only occurs at millimolar concentrations in a manner compatible with nonspecific denaturation, compared with the distinct ordered destabilization induced by micromolar concentrations of fatty acids [51]. As such, the DNP-binding site may not be relevant to fatty acid binding or the reported DNP activity [33].

Second, the reported structure of the DNP-bound UCP1 [17] is in a c-state through the formation of the matrix network and glutamine braces, comprising three ionic and two hydrogen bonds (Figure 4C) [16]. This matrix network arrangement is similar to those of the unliganded and purine nucleotide-bound states (Figure 4C), which do not conduct protons [3]. Therefore, it is unlikely

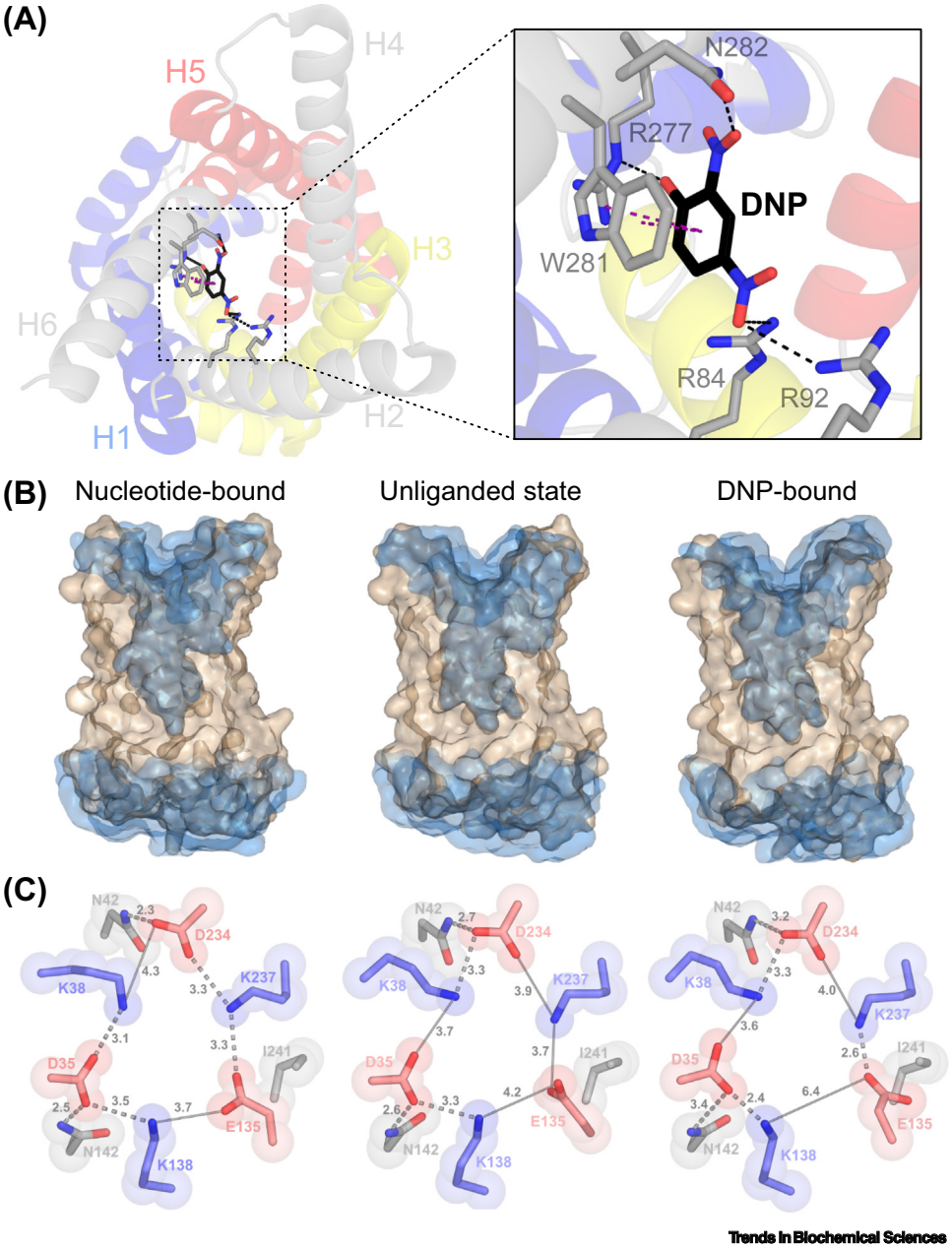

Figure 4. The dinitrophenol-bound structure does not reveal an activated state. (A) Cytoplasmic view of uncoupling protein 1 (UCP1) bound to 2,4-dinitrophenol (DNP). Core elements are colored by domain in blue, yellow, and red, and gate elements are in gray. Insert shows the DNP-binding site, black dashes represent hydrogen bonds and purple dashes represent π-π stacking. (B) Cross-section of the surface view of nucleotide-bound (PDB ID: 8G8W chain A), unliganded (PDB ID: 8HBV chain A), and DNP-bound (PDB ID: 8J1N chain A) UCP1 states. The blue semitransparent surfaces reveal the internal cavities. (C) Matrix gate of the nucleotide-bound (left), unliganded (center), and DNP-bound (right) UCP1 states. Positively charged residues are in blue, negatively charged residues are in red, and neutral residues are in gray. Broken lines show polar interactions and thin gray lines represent distances between non-interacting residues.

that thermal energy is sufficient to break this bonding arrangement. In the related mitochondrial ADP/ATP carrier, which has a weaker interaction network, conformational changes only occur upon substrate binding [52], explaining the equimolar adenine nucleotide exchange [53]. Here,

the structure clearly shows that DNP binding does not provide sufficient energy input to break the networks. Any shift to a proton permeable state without breaking the network in an unrelated mechanism would likely require significant novel features in UCP1 distinct from other mitochondrial carriers, although none are apparent [54].

Third, many of the residues interacting with DNP in UCP1, for example, key residues W281, R92, and N282, are not conserved in the mitochondrial ADP/ATP carrier, which has also been proposed as a facilitator for DNP-induced uncoupling [33]. The UCP1 site is situated between H2 and H6 (Figure 4A), whereas the binding site of DNP proposed for the ADP/ATP carrier based on molecular dynamics simulations is between H4 and H5 [33].

In conclusion, DNP binding does not provide evidence for any activation mechanism. The binding is extremely weak, does not induce conformational changes, has insufficient binding energy to release the matrix network and glutamine brace interactions, and is most likely unrelated to fatty acid binding.

UCP1 has all the functional elements for a carrier-like mechanism

As described earlier, all structures of UCP1 are likely to be in a proton-impermeable c-state (Figure 4B), which could be due to the matrix network being stronger compared with the **cytoplasmic network**, increasing the probability of its formation [20]. Indeed, the matrix network is stronger than the cytoplasmic network due to the absence of a salt bridge between H2 and H4 (Figure 5D) [20]. Importantly, for all determined structures, nanobodies or sybodies were used that were selected against the nucleotide-bound state of UCP1 and, thus, could be responsible for maintaining a single conformation.

While some assert that the c-state is the only functional state of UCP1 [17], we believe that the observed changes in proteolysis sensitivity in response to fatty acids have provided evidence that conformational changes are part of the activation mechanism [55,56]. Furthermore, thermostability studies show that UCP1 shifts to a less stable population in response to activators, indicating that some conformational changes accompany activation [37,51,54]. In addition, UCP1 has both salt bridge networks and braces, which are key conserved features in the mechanism of mitochondrial carriers (Figure 5). Moreover, the interaction energy of the cytoplasmic network is even stronger than in many other mitochondrial carriers with an established transport function [20], indicating that formation of an m-state is a conserved property of UCP1 [20].

Vital to the conformational cycle of mitochondrial carriers is the rotation of the even-numbered helices across the surface of odd-numbered helices [23,24]. In addition, the transmembrane helices on the cytoplasmic side need to come close together in the m-state for the formation of the cytoplasmic network [16,24] (Figure 5B,D). Although the m-state structure has not been solved, all small residues in the helical interfaces that allow these movements to occur in other mitochondrial carriers are also present in UCP1, indicating that the ability to cycle between states is likely to be conserved [16]. Finally, the nucleotide-bound structures are in an intermediary rather than a pure c-state [16]. More specifically, the gate element of H2 is rotated into a position closer to that of an m-state, suggesting that UCP1 has retained its ability to convert to the m-state. Notably, the related UCP2 and UCP3 proteins share these functional features and have four-carbon metabolite transport activity [57–59], suggesting that a transport conformational cycle is retained in these related proteins to support their respective functions. Thus, all the sequence and structural data are consistent with the notion that UCP1 is a mitochondrial carrier capable of undergoing conformational changes, similar to those of a transport cycle.

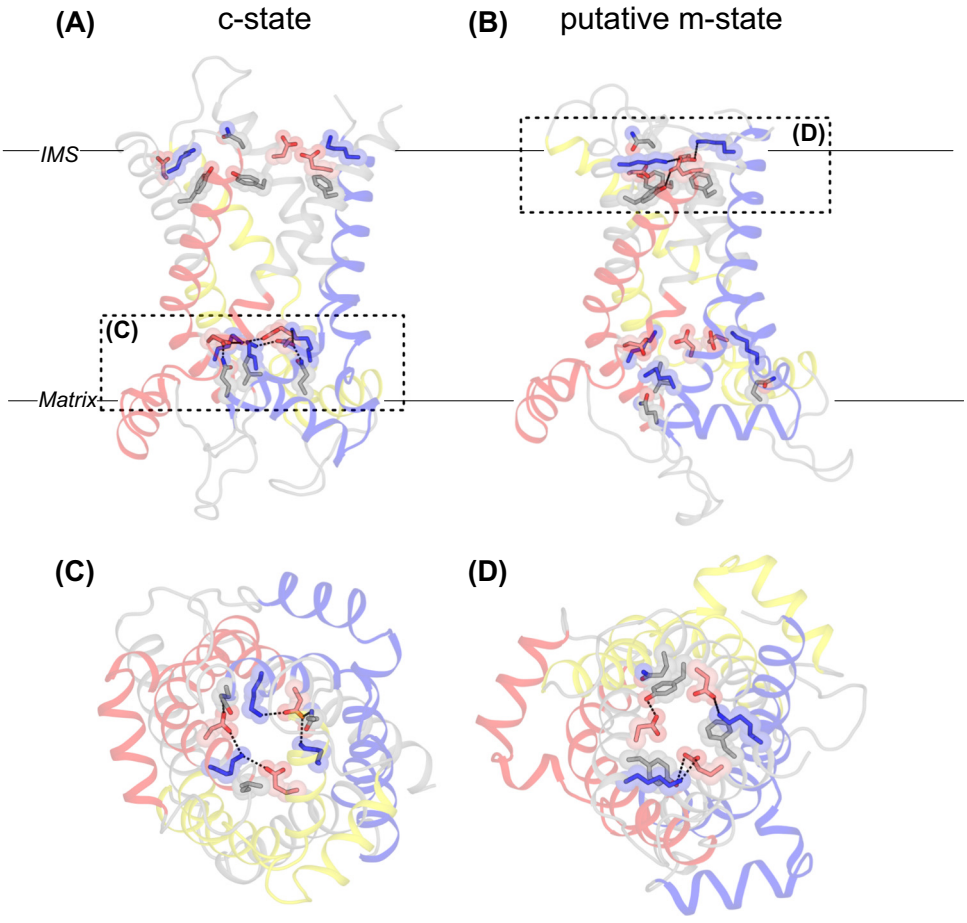

Figure 5. Proposed conformational changes of uncoupling protein 1 (UCP1). (A) Structure of UCP1 in cytoplasmic (c)-state (PDB ID: 8G8W chain A) and (B) a model of UCP1 in the matrix (m)-state based on the m-state of the mitochondrial ADP/ATP carrier (PDB ID: 6GCI, chain A) [24] (C) Matrix-side view of c-state structure of UCP1, showing the matrix gate residues, with interactions between residues shown in black broken lines. Positively charged residues are in blue, negatively charged residues are in red and neutral residues are in gray (D) Cytoplasmic view of the m-state model of UCP1, showing the cytoplasmic gate residues colored as in (C).

Physiological activation of UCP1

The mechanism by which free fatty acids activate UCP1 remains undefined, but four main biochemical models have been proposed [54]. The competition model suggests that fatty acids act merely to remove purine nucleotides from an otherwise intrinsically active protein [60]. The cofactor model proposes that fatty acids become part of the proton conductance pathway, acting as a protonatable group [61]. Two alternative models propose that fatty acids are transport substrates of UCP1. In the shuttling model, fatty acids are transported by UCP1 but remain bound to the protein, chaperoning the proton across the membrane [62]. In the cycling model, fatty acid anions are exported by UCP1, after which the protonated fatty acids flip back across the membrane, independently from the protein, causing a net proton flux across the membrane [63,64]. However, the recently published structural studies have not revealed an activated state [16,17] and, thus, are unable to discriminate between the current proposed models of activation.

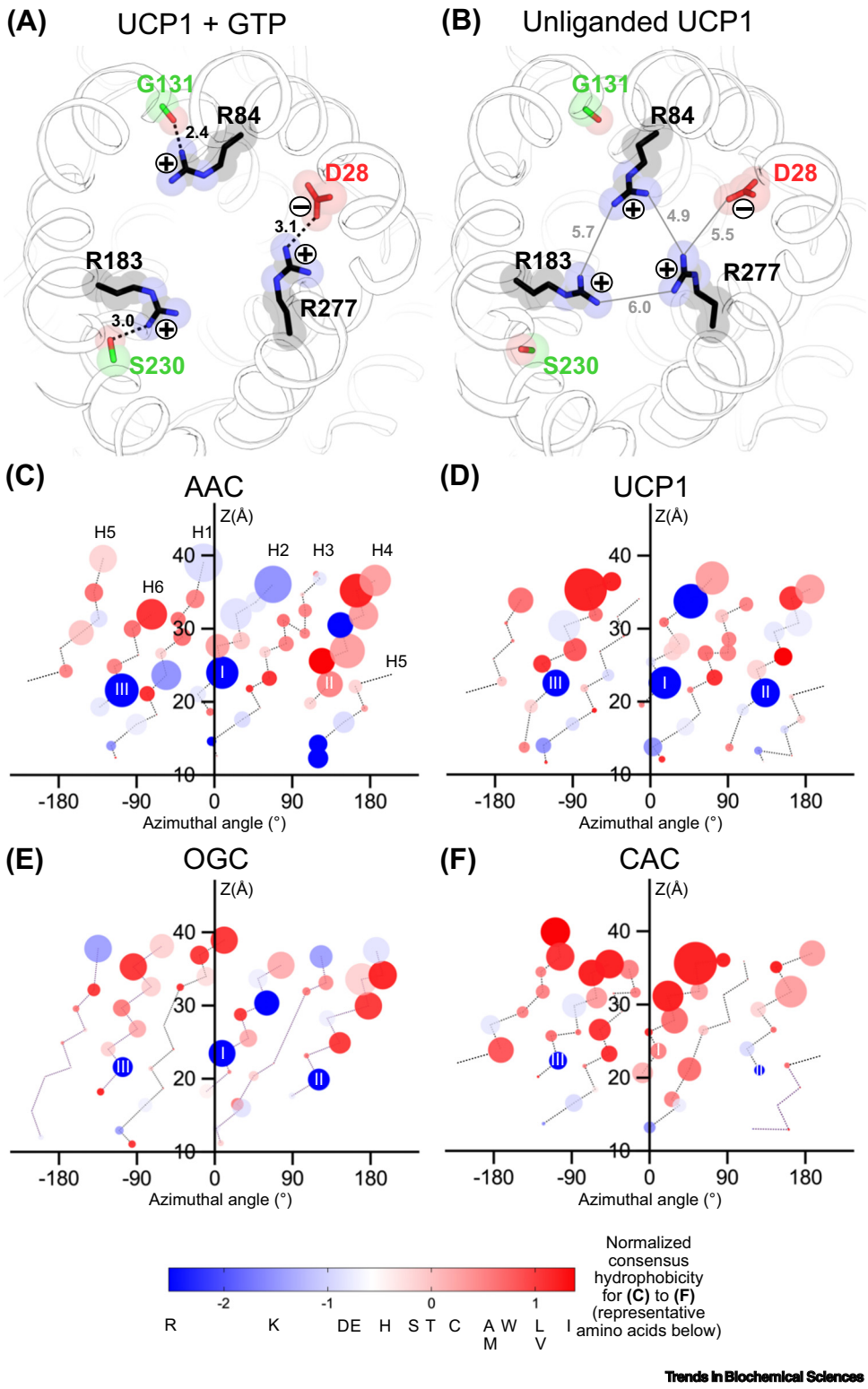

(See figure legend at the bottom of the next page.)

UCP1 likely evolved from the closely related dicarboxylate (DIC) and oxoglutarate (OGC) carriers, which transport their substrates without proton coupling [25]. A direct comparison with these proteins provides insights into how UCP1 might have evolved a proton-translocating function. All three proteins share a similar central substrate-binding site, containing the symmetric arginine triplet R84, R183, R277 at the substrate contact points and Q85 [25]. UCP1-specific adaptations in this site include the negatively charged D28, which has been shown to be important for proton conductance by UCP1 [25,65]. In the nucleotide-bound state, the arginine triplet interacts with other residues: R84 with the carbonyl backbone of G131; R183 with S230; and R277 with D28 (Figure 6A). However, in the nucleotide-free state, these interactions are broken and all three arginine residues point into the central cavity (Figure 6B). Importantly, D28, which was in an ionic bond with R277, is released and, thus, could become available for proton binding. The proposed substrates of UCP1, free fatty acids, are highly hydrophobic, especially when compared with the substrates of dicarboxylate and oxoglutarate carriers. The only mitochondrial carrier that transports substrates with a fatty acyl group is the carnitine/acylcarnitine carrier (CAC) [66]. Comparison of the central cavity residues with respect to hydrophobicity reveals that UCP1 is overall less hydrophobic compared with the carnitine/acylcarnitine carrier and more like the ADP/ATP carrier and dicarboxylate carrier (Figure 6). We believe that this observation suggests that the central cavity of UCP1 has not evolved extensively to enable fatty acid binding as a transport substrate, but does not exclude it. It is likely that UCP1 evolved from dicarboxylate carriers along with the other related UCP2 and UPC3 for a particular anion transport function, such as for small four-carbon metabolites [57–59]. A limited number of subsequent adaptations occurred for its role in thermogenesis [25], as a late evolutionary development, consistent with phylogenetic analysis [67,68]. Further studies of UCP1 activation, both structural and functional, will be required to determine how UCP1 activates thermogenesis.

Concluding remarks

The structures of human UCP1 in the nucleotide-bound and free state represent a major advance in understanding the molecular mechanism of UCP1 inhibition in non-shivering thermogenesis. Comparison of both states shows how purine nucleotides inhibit UCP1 in a pH-dependent manner. While the molecular mechanism of activation of UCP1 remains unresolved, several potential elements have been uncovered, such as the release of the arginine triplet and D28, the presence of networks and braces, the conservation of small interhelical residues, and the partial conformational changes, indicative of state interconversion as part of the activation mechanism. However, many questions remain (see Outstanding questions), in particular how UCP1 is activated *in vivo* by free fatty acids. A molecular understanding of how fatty acids initiate proton leak across the mitochondrial inner membrane by UCP1 will provide an improved mechanistic understanding of non-shivering thermogenesis in humans and offer potential therapeutic strategies for addressing metabolic disorders.

Figure 6. Substrate-binding site area of mitochondrial carriers. (A) Contact point residues of uncoupling protein 1 (UCP1) inhibited with GTP (PDB ID: 8G8W chain A). Black broken lines represent hydrogen bonds with distance in angstrom labeled. (B) Contact point residues of UCP1 free state (PDB ID: 8HBV chain A). Gray lines show distance in angstrom between arginine residues. (C) Cα atoms of residues lining the cavity of bovine ADP/ATP carrier (AAC) (PDB ID: 1OKC) [22], (D) human UCP1 (PDB ID: 8HBV chain A) [17], (E) *Tetrahymena thermophila* oxoglutarate carrier (OGC) (PDB ID: 7W5Z chain M2) [69], and (F) human carnitine/acylcarnitine carrier (CAC) AlphaFold homology model (PDB ID: AF-O43772-F1-model_v4.pdb). (C–F) 2D projections of the cavity-lining residues, viewed from the center of the cavity. Each Cα atom is represented as a sphere at its appropriate azimuthal angle and Z-height above a plane perpendicular to the longitudinal axis. The sphere area is proportional to the solvent-accessible surface area of the residue (calculated by AREAIMOL [70]), and the color represents the normalized consensus hydrophobicity of the residue [71], where red is the most hydrophobic and blue the most hydrophilic. Cavity-lining residues lie on transmembrane helices, indicated by the dotted lines, and labeled in (C). Contact point residues are labeled I, II, and III.

Outstanding questions

Where in the structure of UCP1 do fatty acid activators bind and how do they activate? Do fatty acids act as transport substrates or cofactors?

What conformational changes are required to activate UCP1 proton conductance. Is there a specific activated state, or does UCP1 use a dynamic mechanism?

How do fatty acids overcome purine nucleotide inhibition during activation, when purine nucleotides are present at millimolar concentrations in the cytoplasm?

How do various purine nucleotide species in the cell compete to influence regulation of UCP1? Are there UCP1 isoform-specific adaptations?

Does UCP1 cycle between a c-state and m-state for proton leak activity, as observed for the metabolite transport cycle of other SLC25 family members, or are these states used for a similar, but so far unknown, metabolite transport function of UCP1?

What specific molecular adaptations has UCP1 acquired to facilitate proton leak and thermogenesis? Do these occur in other carriers and bestow a related proton conductance activity?

What biochemical and physiological function do other uncoupling proteins have (UCP2–5)? Understanding whether these related proteins also cause mitochondrial uncoupling may help to reveal the mechanism of activation.

Do purine nucleotides inhibit other mitochondrial carriers? Multiple conserved residues in the central cavity between UCP1 and related proteins suggest similar regulatory mechanisms.

What is the physiological activation mechanism of UCP1? Do other endogenous molecules, in addition to fatty acids, activate *in vivo*, related to other physiological stimuli, such as in response to eating?

Can we develop novel pharmacological agents that specifically target UCP1 *in vivo* and enhance its thermogenic

activity? Are there molecules that can activate both brown adipocyte proliferation and UCP1 directly in the absence of physiological stimuli?

Acknowledgments

We would like to acknowledge financial support from the UKRI Medical Research Council (MC_UU_00028/2) and Biotechnology and Biological Sciences Research Council (BB/S00940X/1).

Declaration of interests

None declared by authors.

References

1. Lidell, M.E. (2019) Brown adipose tissue in human infants. *Handb. Exp. Pharmacol.* 251, 107–123
2. Harms, M. and Seale, P. (2013) Brown and beige fat: development, function and therapeutic potential. *Nat. Med.* 19, 1252–1263
3. Nicholls, D.G. (2021) Mitochondrial proton leaks and uncoupling proteins. *Biochim. Biophys. Acta Bioenerg.* 1862, 148428
4. Rial, E. *et al.* (1983) Brown-adipose-tissue mitochondria: the regulation of the 32 000-Mr uncoupling protein by fatty acids and purine nucleotides. *Eur. J. Biochem.* 137, 197–203
5. Heaton, G.M. *et al.* (1978) Brown-adipose-tissue mitochondria: photoaffinity labelling of the regulatory site of energy dissipation. *Eur. J. Biochem.* 82, 515–521
6. Klingenberg, M. (1988) Nucleotide binding to uncoupling protein. Mechanism of control by protonation. *Biochemistry* 27, 781–791
7. Shih, M.F. and Taberner, P.V. (1995) Selective activation of brown adipocyte hormone-sensitive lipase and cAMP production in the mouse by β3-adrenoceptor agonists. *Biochem. Pharmacol.* 50, 601–608
8. Locke, R.M. *et al.* (1982) Fatty acids as acute regulators of the proton conductance of hamster brown-fat mitochondria. *Eur. J. Biochem.* 129, 373–380
9. Nicholls, D.G. (2017) The hunt for the molecular mechanism of brown fat thermogenesis. *Biochimie* 134, 9–18
10. Stanford, K.I. *et al.* (2013) Brown adipose tissue regulates glucose homeostasis and insulin sensitivity. *J. Clin. Invest.* 123, 215–223
11. Bartelt, A. *et al.* (2011) Brown adipose tissue activity controls triglyceride clearance. *Nat. Med.* 17, 200–206
12. Nedergaard, J. *et al.* (2007) Unexpected evidence for active brown adipose tissue in adult humans. *Am. J. Physiol. Endocrinol. Metab.* 293, E444–E452
13. Cypess, A.M. *et al.* (2009) Identification and importance of brown adipose tissue in adult humans. *N. Engl. J. Med.* 360, 1509
14. Saito, M. *et al.* (2009) High incidence of metabolically active brown adipose tissue in healthy adult humans: effects of cold exposure and adiposity. *Diabetes* 58, 1526
15. Chondronikola, M. *et al.* (2014) Brown adipose tissue improves whole-body glucose homeostasis and insulin sensitivity in humans. *Diabetes* 63, 4089–4099
16. Jones, S.A. *et al.* (2023) Structural basis of purine nucleotide inhibition of human uncoupling protein 1. *Sci. Adv.* 9, eadh425
17. Kang, Y. and Chen, L. (2023) Structural basis for the binding of DNP and purine nucleotides onto UCP1. *Nature* 620, 226–231
18. Kunji, E.R.S. *et al.* (2020) The SLC25 carrier family: Important transport proteins in mitochondrial physiology and pathology. *Physiology* 35, 302–327
19. Ruprecht, J.J. and Kunji, E.R. (2019) Structural changes in the transport cycle of the mitochondrial ADP/ATP carrier. *Curr. Opin. Struct. Biol.* 57, 135–144
20. Ruprecht, J.J. and Kunji, E.R.S. (2020) The SLC25 mitochondrial carrier family: structure and mechanism. *Trends Biochem. Sci.* 45, 244–258
21. Ruprecht, J.J. and Kunji, E.R.S. (2021) Structural mechanism of transport of mitochondrial carriers. *Annu. Rev. Biochem.* 20, 535–558
22. Pebay-Peyroula, E. *et al.* (2003) Structure of mitochondrial ADP/ATP carrier in complex with carboxyatractyloside. *Nature* 426, 39–44
23. Ruprecht, J.J. *et al.* (2014) Structures of yeast mitochondrial ADP/ATP carriers support a domain-based alternating-access transport mechanism. *Proc. Natl. Acad. Sci. USA* 111, E426–E434
24. Ruprecht, J.J. *et al.* (2019) The molecular mechanism of transport by the mitochondrial ADP/ATP carrier. *Cell* 176, 435–447
25. Robinson, A.J. *et al.* (2008) The mechanism of transport by mitochondrial carriers based on analysis of symmetry. *Proc. Natl. Acad. Sci. USA* 105, 17766–17771
26. Kunji, E.R.S. and Robinson, A.J. (2006) The conserved substrate binding site of mitochondrial carriers. *Biochim. Biophys. Acta Bioenerg.* 1757, 1237–1248
27. Robinson, A.J. and Kunji, E.R.S. (2006) Mitochondrial carriers in the cytoplasmic state have a common substrate binding site. *Proc. Natl. Acad. Sci. USA* 103, 2617–2622
28. Wentinck, K. *et al.* (2022) Putting on molecular weight: enabling cryo-EM structure determination of sub-100-kDa proteins. *Curr. Res. Struct. Biol.* 4, 332
29. Uchański, T. *et al.* (2020) Nanobodies to study protein conformational states. *Curr. Opin. Struct. Biol.* 60, 117–123
30. Pardon, E. *et al.* (2014) A general protocol for the generation of nanobodies for structural biology. *Nat. Protoc.* 9, 674–693
31. Botte, M. *et al.* (2022) Cryo-EM structures of a LptDE transporter in complex with Pro-macrobodies offer insight into lipopolysaccharide translocation. *Nat. Commun.* 13, 1826
32. Wu, X. and Rapoport, T.A. (2021) Cryo-EM structure determination of small proteins by nanobody-binding scaffolds (Legobodies). *Proc. Natl. Acad. Sci. USA* 118, e2115001118
33. Bertholet, A.M. *et al.* (2022) Mitochondrial uncouplers induce proton leak by activating AAC and UCP1. *Nature* 606, 180–187
34. Lee, Y. *et al.* (2015) Uncoupling protein 1 binds one nucleotide per monomer and is stabilized by tightly bound cardiolipin. *Proc. Natl. Acad. Sci. USA* 112, 6973–6978
35. Lin, C.S. and Klingenberg, M. (1982) Characteristics of the isolated purine nucleotide binding protein from brown fat mitochondria. *Biochemistry* 21, 2950–2956
36. Mavridou, V. *et al.* (2022) Substrate binding in the mitochondrial ADP/ATP carrier is a step-wise process guiding the structural changes in the transport cycle. *Nat. Commun.* 13, 3585
37. Crichton, P.G. *et al.* (2015) Trends in thermostability provide information on the nature of substrate, inhibitor, and lipid interactions with mitochondrial carriers. *J. Biol. Chem.* 290, 8206–8217
38. Kumar, P. *et al.* (2015) Dissecting p-helices: sequence, structure and function. *FEBS J.* 282, 4415–4432
39. Echtay, K.S. *et al.* (2018) Uncoupling proteins: Martin Klingenberg's contributions for 40 years. *Arch. Biochem. Biophys.* 657, 41–55
40. Winkler, E. *et al.* (1997) Identification of the pH sensor for nucleotide binding in the uncoupling protein from brown adipose tissue. *Biochemistry* 36, 148–155
41. Echtay, K.S. *et al.* (1997) Mutagenesis of the uncoupling protein of brown adipose tissue. Neutralization of E190 largely abolishes pH control of nucleotide binding. *Biochemistry* 36, 8253–8260
42. Shuvalov, V.A. *et al.* (1988) Nucleotide binding to uncoupling protein. Mechanism of control by protonation? *Proc. Natl. Acad. Sci. USA* 27, 3830–3832
43. Echtay, K.S. *et al.* (2001) Role of intrahelical arginine residues in functional properties of uncoupling protein (UCP1). *Biochemistry* 40, 5243–5248
44. Klingenberg, M. (2017) UCP1 - a sophisticated energy valve. *Biochimie* 134, 19–27
45. Klingenberg, M. and Huang, S.-G. (1999) Structure and function of the uncoupling protein from brown adipose tissue. *Biochim. Biophys. Acta* 1415, 271–296
46. Gagelin, A. *et al.* (2023) Molecular determinants of inhibition of UCP1-mediated respiratory uncoupling. *Nat. Commun.* 14, 2594
47. McLaughlin, S.G.A. and Dilger, J.P. (1980) Transport of protons across membranes by weak acids. *Physiol. Rev.* 60, 825–863

48. Colman, E. (2007) Dinitrophenol and obesity: an early twentieth-century regulatory dilemma. *Regul. Toxicol. Pharmacol.* 48, 115–117
49. Grundlingh, J. *et al.* (2011) 2,4-Dinitrophenol (DNP): a weight loss agent with significant acute toxicity and risk of death. *J. Med. Toxicol.* 7, 205
50. Siegmueller, C. and Narasimhaiah, R. (2010) Fatal 2,4-dinitrophenol poisoning… coming to a hospital near you. *Emerg. Med. J.* 27, 639–640
51. Cavalieri, R. *et al.* (2022) Activating ligands of Uncoupling protein 1 identified by rapid membrane protein thermostability shift analysis. *Mol. Metab.* 62, 101526
52. Springett, R. *et al.* (2017) Modelling the free energy profile of the mitochondrial ADP/ATP carrier. *Biochim. Biophys. Acta Bioenerg.* 1858, 906–914
53. Pfaff, E. *et al.* (1965) Unspecific permeation and specific exchange of adenine nucleotides in liver mitochondria. *Biochim. Biophys. Acta Gen. Subj.* 104, 312–315
54. Crichton, P.G. *et al.* (2017) The molecular features of uncoupling protein 1 support a conventional mitochondrial carrier-like mechanism. *Biochimie* 134, 35–50
55. Huang, S.G. (2003) Limited proteolysis reveals conformational changes in uncoupling protein-1 from brown adipose tissue mitochondria. *Arch. Biochem. Biophys.* 420, 40–45
56. Divakaruni, A.S. *et al.* (2012) Fatty acids change the conformation of uncoupling protein 1 (UCP1). *J. Biol. Chem.* 287, 36845–36853
57. Vozza, A. *et al.* (2014) UCP2 transports C4 metabolites out of mitochondria, regulating glucose and glutamine oxidation. *Proc. Natl. Acad. Sci. USA* 111, 960–965
58. Kreiter, J. *et al.* (2023) Uncoupling protein 3 catalyzes the exchange of C4 metabolites similar to UCP2. *Biomolecules* 14, 21
59. De Leonardis, F. *et al.* (2024) Human mitochondrial uncoupling protein 3 functions as a metabolite transporter. *FEBS Lett.* 598, 338–346
60. Shabalina, I.G. *et al.* (2004) Native UCP1 displays simple competitive kinetics between the regulators purine nucleotides and fatty acids. *J. Biol. Chem.* 279, 38236–38248
61. Winkler, E. and Klingenberg, M. (1994) Effect of fatty acids on H+ transport activity of the reconstituted uncoupling protein. *J. Biol. Chem.* 269, 2508–2515
62. Fedorenko, A. *et al.* (2012) Mechanism of fatty-acid-dependent UCP1 uncoupling in brown fat mitochondria. *Cell* 151, 400–413
63. Garlid, K.D. *et al.* (1998) The mechanism of proton transport mediated by mitochondrial uncoupling proteins. *FEBS Lett.* 438, 10–14
64. Garlid, K.D. *et al.* (1996) On the mechanism of fatty acid-induced proton transport by mitochondrial uncoupling protein. *J. Biol. Chem.* 271, 2615–2620
65. Echtay, K.S. *et al.* (2000) Site-directed mutagenesis identifies residues in uncoupling protein (UCP1) involved in three different functions. *Biochemistry* 39, 3311–3317
66. Tonazzi, A. *et al.* (2021) The mitochondrial carnitine acyl-carnitine carrier (SLC25A20): molecular mechanisms of transport, role in redox sensing and interaction with drugs. *Biomolecules* 11, 521
67. Hughes, D.A. *et al.* (2009) Molecular evolution of UCP1 and the evolutionary history of mammalian non-shivering thermogenesis. *BMC Evol. Biol.* 9, 4
68. Gaudry, M.J. *et al.* (2019) Molecular evolution of thermogenic uncoupling protein 1 and implications for medical intervention of human disease. *Mol. Asp. Med.* 68, 6–17
69. Zhou, L. *et al.* (2022) Structures of Tetrahymena's respiratory chain reveal the diversity of eukaryotic core metabolism. *Science* 376, 831–839
70. Winn, M.D. *et al.* (2011) Biological crystallography overview of the CCP4 suite and current developments. *Acta Crystallogr. D Biol. Crystallogr.* 67, 235–242
71. Eisenberg, D. *et al.* (1984) Analysis of membrane and surface protein sequences with the hydrophobic moment plot. *J. Mol. Biol.* 179, 125–142